

# Simulation of chiral topological phases in driven quantum dot arrays

Beatriz Pérez-González,\* Miguel Bello, Gloria Platero, and Álvaro Gómez-León  
*Instituto de Ciencia de Materiales de Madrid (ICMM-CSIC)*

(Dated: November 27, 2021)

We discuss how to use quantum dot arrays as quantum simulators for 1D chiral topological phases. We show that by driving the system out of equilibrium with a particular driving protocol, one can modify the hopping amplitudes at will, imprinting bond-order to the lattice and thus effectively producing structures such as dimers, trimers, etc. Our driving protocol also allows for the simultaneous suppression of all the undesired hopping processes, the enhancement of the necessary ones, and then provides a way to maintain certain key symmetries which provide topological protection. In addition, we have discussed its implementation in a 12-QD array with two interacting electrons, and found correlation effects in their dynamics when configurations with different number of edge states are considered.

*Introduction.* Topological phases of matter constitute an active field of research due to their tantalizing physical properties and to their promising technological applications, such as quantum computation [1–3], quantum information [4], spintronics [5, 6] and magnetic devices [7]. Of all topological matter, topological insulators (TIs) [8–10] are of special interest due to the presence of topologically protected surface or edge states, robust to local perturbations. Despite the numerous experimental observations of topological fingerprints in different materials [11–16], the need for a careful band structure engineering and the limited tunability in samples are restraining factors in the search for TIs. As a consequence, a great effort is being made to simulate the behaviour of TIs by tailoring other quantum systems, whose properties can be controlled more easily. Within this context, time-dependent modulations have proven to be useful tools to modify the topology and the electronic properties of the system [17–28]. Particularly, they have been used to simulate the behaviour of TIs, giving rise to the so-called “Floquet topological insulators” (FTIs) [29–31] upon different systems [31–50].

In the solid-state community, quantum dots (QDs) have revealed themselves as highly tunable and controllable quantum systems [51, 52], in which both on-site energies [53] and couplings [54, 55] can be addressed independently. This makes them an interesting platform for quantum simulation [56–58]. Recent experimental evidence on scalable quantum dot devices [59] demonstrates a reproducible and controllable 12-quantum-dot device. This achievement opens up the possibility of simulating 1D TIs in quantum dot chains.

In this work we show that a quantum simulator for 1D chiral topological phases can be obtained by periodically driving an array of QDs with long-range hopping. We propose a driving protocol which enables us to imprint bond-order in the lattice [60], while also offers tunability of the long-range hoppings. This control can be used to tune the hopping amplitudes to configurations that would be unreachable otherwise, while preserving the fundamental symmetries which guarantee topological

features. Thus, the driving protocol triggers topological behaviour in a trivial setup, opening the door to the simulation of different chiral topological phases. Furthermore, we also study the exact time-evolution for the case of two interacting electrons, and show that the dynamics of different edge states modes can become highly correlated. This allows to discriminate between different topological phases and also opens up new possibilities for quantum state transfer protocols.

*Model.* We consider a Hamiltonian describing a driven chain of QDs:

$$H(t) = \sum_{|i-j| \leq R} J_{ij} c_i^\dagger c_j + \sum_i A_i f(t) c_i^\dagger c_i \quad (1)$$

$$\equiv H_{\text{array}} + H_{\text{driv}}(t),$$

where  $c_i^\dagger$  ( $c_i$ ) is the creation (destruction) operator for a spin-less fermion at the  $i^{\text{th}}$  site of the array. The first term represents the static Hamiltonian for a QD array of  $N$  sites, with  $J_{ij}$  being the real hopping amplitude connecting the  $i^{\text{th}}$  and  $j^{\text{th}}$  dots. Note that long-range hoppings are allowed to take place, up to range  $R$ . We will assume that hopping amplitudes in the undriven system decay monotonically as a function of the distance between sites,  $J_{ij} = J(|i - j|)$ . The second term in Eq. (1),  $H_{\text{driv}}(t)$ , corresponds to a time-periodic modulation of the on-site potentials  $A_i$  with  $f(t) = f(T + t)$ , and frequency  $\omega = 2\pi/T$ .

Regarding the simulation of chiral topological phases in QD arrays, the purpose of the time-periodic modulation is threefold: First, the driving must generate bond order, which is a crucial ingredient in toy models such as the SSH [61]. Second, we seek to enforce chiral symmetry within these effective periodic lattices, which means that even-neighbor hoppings must be simultaneously suppressed through the so-called coherent destruction of tunneling [62, 63] (even/odd hopping refers to the case when the hopping is between the same/different sub-lattice sites, respectively). This unrealistic requirement turns out to be feasible when a driving protocol is included.

Finally, odd long-range hoppings must be enhanced with respect to short-range ones in order to obtain certain topological phases beyond those appearing with merely first-neighbor couplings.

All these objectives can be achieved through a square ac field

$$f(t) = \begin{cases} 1 & \text{if } 0 \leq t < T/2 \\ -1 & \text{if } T/2 \leq t < T \end{cases}, \quad (2)$$

and in particular, the simulation of an effective dimer lattice with long-range hopping can be realized by choosing the  $A_i$  in a stair-like fashion,

$$A_{2n} = n(\alpha + \beta), \quad A_{2n-1} = n(\alpha + \beta) - \alpha. \quad (3)$$

with  $n = 1, 2, 3, \dots$ , which translates into an alternating difference between two consecutive sites, namely  $A_{2n} - A_{2n-1} = \alpha$  and  $A_{2n+1} - A_{2n} = \beta$ . Given the time-periodicity of the Hamiltonian  $H(t) = H(t + T)$  [64, 65], we can take advantage of Floquet theory to solve the time-dependent Schrödinger equation. The solutions take the form  $|\psi_n(t)\rangle = e^{-i\epsilon_n t} |u_n(t)\rangle$ , where the so-called Floquet modes  $|u_n(t)\rangle = |u_n(t + T)\rangle$  have the same periodicity as the Hamiltonian, and  $\epsilon_n$  are the so-called quasienergies, which play an analogous role to the energies in the static Hamiltonians. In the high-frequency regime ( $\omega \gg J_0$ ), the dynamics is essentially dictated by the stroboscopic evolution of an effective time-independent Hamiltonian  $H_{\text{eff}}$ , which can be derived with a Magnus expansion. This leads to an effective Hamiltonian which is identical to  $H_{\text{array}}$ , but with renormalized hopping amplitudes (see Appendix ??):

$$J_{ij} \rightarrow \tilde{J}_{ij} = J_{ij} \frac{i\omega}{\pi(A_i - A_j)} \left( e^{-i\pi(A_i - A_j)/\omega} - 1 \right). \quad (4)$$

From Equation (4) we can see that even-neighbor hoppings  $J_{i,i\pm 2m}$  with  $m = 1, 2, 3, \dots$  ( $\pm$  for hoppings to the right and left, respectively) renormalize through  $A_i - A_{i\pm 2m} = \mp m(\alpha + \beta)$ . The quenching of all  $\tilde{J}_{i,i\pm 2m}$  can be achieved by simultaneously choosing  $\alpha + \beta = 2\omega q$ , with  $q = 1, 2, 3, \dots$ . Hence, chiral symmetry is recovered, independently of the maximum range of the hoppings included.

On the other hand, the renormalization of the odd-neighbor hoppings leads to bond ordering, due to the alternating structure of the driving protocol. Together with the presence of chiral symmetry, this ensures the existence of distinct topological phases. We identify the renormalized  $J_{2i,2i-r}$  as  $\tilde{J}'_{-r}$  and  $J_{2i+r,2i}$  as  $\tilde{J}_r$  ( $r \in [1, 3, 5, \dots, R]$ ), obtaining

$$\begin{aligned} \tilde{J}'_{-r} &= \frac{iJ_{2i,2i-r}}{\pi[\frac{\omega}{2} + (r-1)q]} \left[ e^{-i\pi(\frac{\omega}{2} + (r-1)q)} - 1 \right], \\ \tilde{J}_r &= \frac{iJ_{2i+r,2i}}{\pi[(r+1)q - \frac{\omega}{2}]} \left[ e^{-i\pi((r+1)q - \frac{\omega}{2})} - 1 \right]. \end{aligned} \quad (5)$$

Notice that now long-range odd-hoppings can be tuned, while keeping even-hoppings suppressed. This can make long-range hoppings dominate over short-range ones, and then allows to explore different topological phases by just tuning the driving amplitudes. The sign of  $r$  in the subscript is relevant since hopping amplitudes are now complex functions, and hence  $\tilde{J}_{\pm r}^{(i)} = (\tilde{J}_{\mp r}^{(i)})^*$ .

Interestingly, our protocol can be generalized to reproduce different kinds of bond-ordering and to enforce other symmetries as well by choosing the driving on-site amplitudes accordingly. A trimer chain [66] is an particular example of a 1D system hosting non-trivial topological phases that can be realized in our set up. In this case, chiral symmetry is intrinsically absent, but the presence of another crystalline symmetry, space-inversion symmetry, can provide for topological protection [67]. A trimer chain can be realized in a QD driven monomer chain just by considering  $A_{2n} - A_{2n-1} = A_{2n+1} - A_{2n} = \alpha$  and  $A_{2n+2} - A_{2n+1} = \beta$ .

*Topological phase diagram for driven QD arrays.* In QD arrays, the bare hopping amplitudes typically decay exponentially with distance, with a decay length  $\lambda$ :  $J_{ij} = J_0 e^{-d_{ij}/\lambda}$ , where  $d_{ij}$  is the distance between the  $i^{\text{th}}$  and  $j^{\text{th}}$  dots and  $J_0$  is of the order of tens of  $\mu\text{eV}$ , which are the typical energy scales in these setups. The distance between two consecutive QDs is set to  $a = 1/2$  so that the unit cell in the effective dimerized chain is 1. By varying the value of  $\alpha$  and  $\lambda$  in the driven system, topological phases with different topological invariant can be realized (Fig.1). The topological invariant  $\mathcal{W}$  is calculated as the winding number of the Bloch vector  $\vec{d}(k) = (\text{Re}[d(k)], -\text{Im}[d(k)])$  around the origin [68], assuming a system with periodic boundary conditions, with  $d(k)$  defined as

$$d(k) = \sum_{r=1}^R \left( \tilde{J}'_{-r} e^{ik \frac{r-1}{2}} + \tilde{J}_{+r} e^{-ik \frac{r+1}{2}} \right), \quad (6)$$

For small values of  $\lambda$ , only  $\mathcal{W} = 1$  and  $\mathcal{W} = 0$  phases are allowed for all values of  $\alpha/w$ , since first-neighbour hoppings are dominant (this corresponds to the SSH model). Then, when  $\lambda$  is increased, other phases with larger  $\mathcal{W}$  are possible, as a function of the ratio  $\alpha/w$  (we have also calculated the size of the gap in the Appendix, as one is typically interested in gap sizes smaller than the temperature of the setup).

Typically, other driving protocols have been considered in the literature, such as sinusoidal driving fields

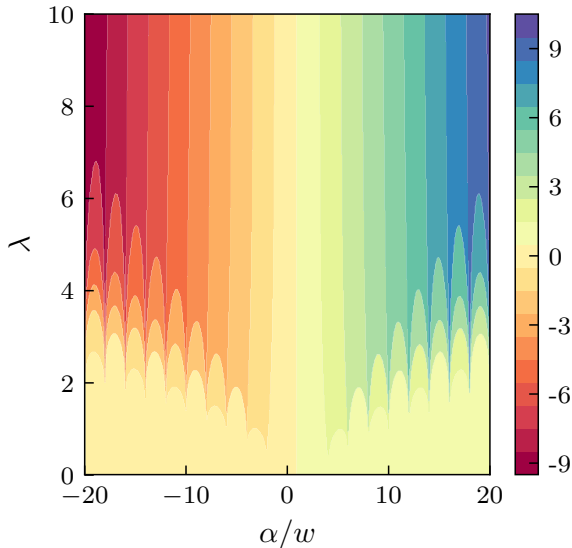


FIG. 1: Topological invariant  $\mathcal{W}$  as a function of the driving amplitude  $\alpha/w$  and decay length of hopping amplitudes  $\lambda$ , for  $q = 1$ . The maximum range of the hoppings included is fixed by  $\lambda$ , such that the longest bare hopping amplitude is a factor  $10^{-8}$  smaller than the shortest one.

$f(t) = \sin(\omega t + \phi)$  [21, 23, 24, 40], or standing waves  $f(t) = \cos(\omega t) \sum_{j=1}^N \cos(kx_j + \phi)$  [69]. However, none of them would be suitable for engineering arbitrary chiral topological phases. In both previous cases, renormalization of the hopping amplitudes occurs through a zero-order Bessel function, whose roots are not periodically spaced. Hence, it would not be possible to suppress all even hoppings at once, and chiral symmetry would not be present. On the other hand, a homogeneous square driving field with  $A_i = A$  could restore chiral symmetry in a dimerized chain but cannot generate topological phases beyond those with  $\mathcal{W} = 0, 1$  if hoppings decay exponentially with distance.

The experimental evidence provided in [59] demonstrates a reproducible and controllable 12-quantum-dot device. Motivated by this experimental setup, we propose the implementation of our driving protocol in an array of 12 quantum dots. In Fig.2 we show the quasienergies, as given by the effective Hamiltonian, of a driven 12-quantum-dot array, as a function of  $\alpha/w$ , with first- and third-neighbor hoppings (second-neighbor hoppings were initially present, but are effectively suppressed by the driving protocol), fixing  $\lambda = 1.5$ . The spectrum shows two topological phases with  $\mathcal{W} = 1$  and  $\mathcal{W} = 2$ .

*Dynamics of two interacting particles.* The number of edge states hosted by a finite system and their localization properties determine the motion of charges along the chain. Then, for an electron initially occupying the

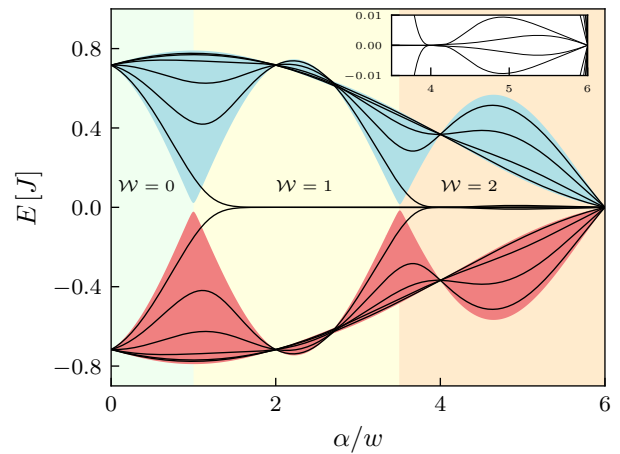


FIG. 2: Quasienergy levels of a driven 12-quantum dot array and band structure in the thermodynamical limit (red and blue filling for the valence and conduction band, respectively), as a function of  $\alpha/w$ , including first- and third- neighbour hoppings, in the high-frequency regime. Second-neighbour hoppings have been suppressed through the driving protocol. The parameters are  $\lambda/w = 1.5$ ,  $q = 1$ . Inset: each pair of edge states in the  $\mathcal{W} = 2$  phase has a different energy splitting, which can be also varied by tuning  $\alpha/w$ .

ending site, one would see oscillations between the two edges of the chain, with a frequency defined by the energy splitting:  $\omega_{\text{osc}} \propto E_+ - E_-$ , being  $E_{\pm}$  the energy of each edge state in the pair. Hence, one can discriminate between topological phases with different number of edge states by studying the electron dynamics.

These ideas are illustrated in Fig.3, where we consider two electrons with opposite spin loaded in a driven array of 12 QDs in such a way that the spin-up (spin-down) particle, which we will denote as  $\uparrow$  ( $\downarrow$ ) initially occupies the first (third) site. In addition we have included a local interaction term, being the total Hamiltonian:

$$H_{\uparrow\downarrow}(t) = \sum_{\sigma} \sum_{|i-j| \leq R} J_{ij} c_{i,\sigma}^{\dagger} c_{j,\sigma} + \sum_{i,\sigma} A_i f(t) n_{i,\sigma} + U \sum_i n_{i,\uparrow} n_{i,\downarrow}, \quad (7)$$

where  $\sigma = \uparrow, \downarrow$ . We do not include any spin-flip terms, since experimental evidence on silicon QDs confirms that the spin relaxation time within these QD structures is very long compared with the other energy scales of the system [70]. The  $A_i$  are chosen as indicated before, and  $\alpha$  is fixed such that the system hosts either two or four edge states. Then the dynamics is exactly calculated from the time evolution operator  $U(t, 0) = e^{-i \int_0^t H_{\uparrow\downarrow} dt}$ . Since  $H_{\uparrow\downarrow}$  is time-independent in each half period, the time-evolution operator  $U(T, 0)$  can be factorized into two in-

dependent time-evolution operators,  $U(T, 0) = U(T) = U_+(\frac{T}{2})U_-(\frac{T}{2})$ , where the subscript  $\pm$  corresponds to the sign of  $f(t)$  in each of them.

First,  $\alpha$  is chosen such that the system hosts one pair of edge states ( $\mathcal{W} = 1$  for the left half of Fig.3), which have the largest weight at the ending sites of the chain. When interaction is turned off, particle  $\uparrow$  oscillates between the ends of the chain, while particle  $\downarrow$  spreads along the chain: at the third site, other states from the bulk have a non-negligible contribution and the edge states do not dominate the dynamics. When  $\alpha$  is fixed so that the system has four edge states ( $\mathcal{W} = 2$  for the right half of Fig.3), one of the pairs is maximally localized at the first and last sites, while the other has the largest weight at the third and second-to-last sites. Hence, each particle is coupled to a different pair of edge states and it displays oscillations between different sites. The frequency of oscillation is also different, since each pair has a different energy splitting (see inset in Fig.2). The second pair has a bigger splitting and thus oscillations for particle  $\downarrow$  happen faster.

Interestingly, for the case of non-vanishing local interaction one can see that the general effect is to correlate the dynamics of the two electrons. For the case of just one pair of edge states, the interaction correlates the edge mode with the bulk. They exchange spectral weight and oscillate coherently. However the case of two pairs of edge modes is more interesting, as the interaction correlates their dynamics, modifying the frequency of the oscillation while maintaining the edge modes isolated from the bulk. Notice that in both cases the frequency of oscillations slightly shifts, which is expected due to the non-linear corrections produced by the interaction.

This difference in the exact dynamics for two particles confirms the method proposed in this work to engineer topological phases and provides a way to characterize them by detecting the time evolution of the charge occupation in the system.

In addition, it is known that the edge states hosted by an SSH finite chain with non-trivial topology allow for long-range transfer of doublons directly from one end to the other without populating the sites in between [17]. Here we show that the two-electron states can be directly transferred between outer dots by considering topological models with a larger winding number. Then, the presence of more pairs of edge states, which can be controlled by choosing a suitable value for  $\alpha/w$ , opens up the possibility of designing new quantum-state-transfer protocols.

## CONCLUSIONS

We have proposed a driving protocol to simulate chiral topological phases in a 1D QDs array. Starting with a chain of QDs and exponentially decaying hoppings, we have shown that our protocol can induce non-trivial

topology in an otherwise trivial setup. This is accomplished when even hoppings are dynamically quenched, while simultaneously odd long-range hoppings are enhanced. Hence chiral symmetry can be restored and the desired bond-order can be enforced by just tuning the amplitude modulation of the on-site energies.

Regarding the experimental implementation of the model, high control of ac driving pulses has been achieved in the last years, and also QD arrays of increasing size have been implemented. Following experimental evidence on scalable quantum dot devices, we recall the architecture employed in [59] with 12 QDs to simulate topological phases with  $\mathcal{W} = 2$ , involving first- to third-neighbour hoppings. Therefore, our set up could be experimentally implemented with the present state of the art regarding control and fabrication of quantum dot arrays. To test the validity of our results we have simulated the exact dynamics for an initial product state, including the effect of local electron interaction. Our result shows that the dynamics can be used to discriminate between the different topological phases. In addition we have found that the interplay of driving and interactions produces a drag effect between the electrons, which leads to the formation of correlated edge modes; this is not only of fundamental interest but also relevant for quantum simulation and information purposes. Interestingly, our driving protocol could also be extended to two-dimensional QDs arrays and other platforms like cold atoms or photonic crystals.

## ACKNOWLEDGEMENTS

This work was supported by the Spanish Ministry of Economy and Competitiveness through Grant MAT2017-86717-P. M. Bello acknowledges the FPI program BES-2015-071573, Á. Gómez-León acknowledges the Juan de la Cierva program and Beatriz Pérez-González acknowledges the FPU program FPU17/05297.

---

\* bperez03@ucm.es

- [1] A. Kitaev, *Annals of Physics* **303**, 2 (2003).
- [2] A. Stern and N. H. Lindner, *Science*, 1179 (2013).
- [3] C. Nayak, S. H. Simon, A. Stern, M. Freedman, and S. Das Sarma, *Rev. Mod. Phys.* **80**, 1083 (2008).
- [4] N. Y. Yao, C. R. Laumann, A. V. Gorshkov, H. Weimer, L. Jiang, J. I. Cirac, P. Zoller, and M. D. Lukin, *Nature Communications* **4**, 1585 EP (2013).
- [5] M. Cinchetti, *Nature Nanotechnology* **9**, 965 EP (2014).
- [6] Y. Fan and K. L. Wang, *World Scientific* **06** (2016), 10.1142/S2010324716400014.
- [7] I. Garate and M. Franz, *Phys. Rev. Lett.* **104**, 146802 (2010).
- [8] C. L. Kane and E. J. Mele, *Phys. Rev. Lett.* **95**, 146802 (2005).

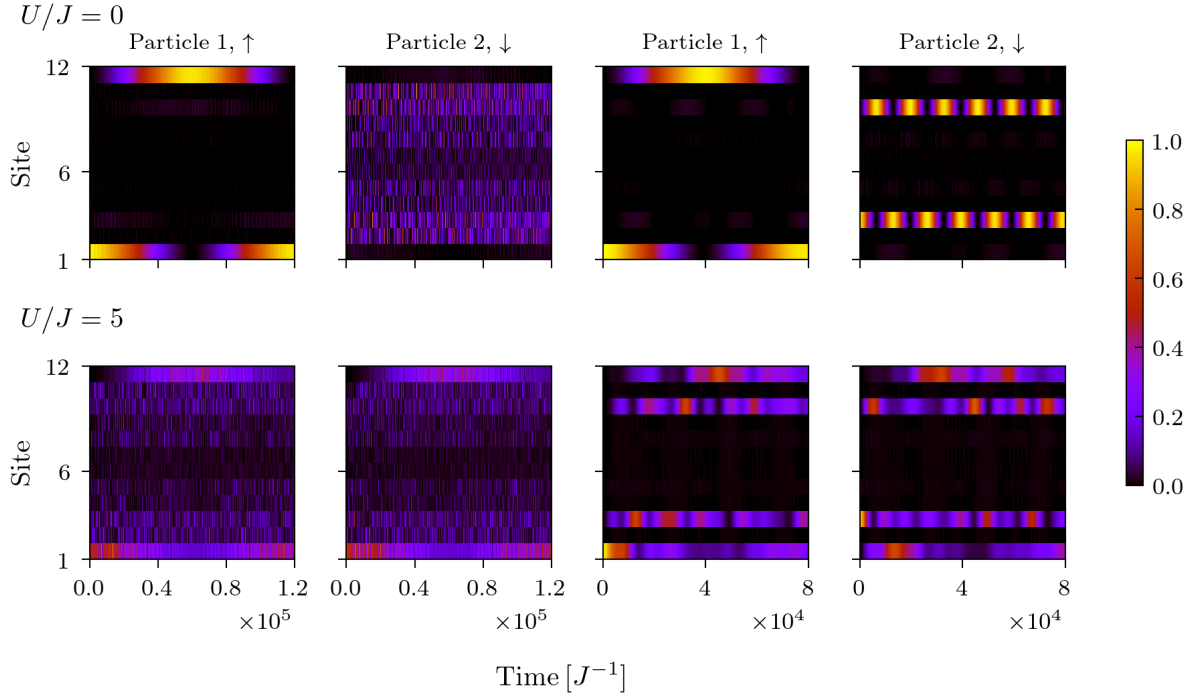


FIG. 3: Occupation of each site of a driven 12-QD array as a function of time when two electrons with opposite spin are loaded into the system, for different values of  $U$ . The array has first- to third-neighbor couplings, whose values initially decay exponentially with distance, choosing  $\lambda = 1.5$ . Considering the high-frequency regime with  $w = 100$  and  $q = 1$ , the values for  $\alpha$  have been chosen such that the desired hopping renormalization is realized. The four left plots correspond to  $\alpha = 230$ , resulting in a topological phase with  $\mathcal{W} = 1$  (two edge states). The four right plots correspond to  $\alpha = 410$ , yielding a configuration with  $\mathcal{W} = 2$  (four edge states)

- [9] M. Z. Hasan and C. L. Kane, Rev. Mod. Phys. **82**, 3045 (2010).
- [10] X.-L. Qi and S.-C. Zhang, Rev. Mod. Phys. **83**, 1057 (2011).
- [11] D. Hsieh, D. Qian, L. Wray, Y. Xia, Y. S. Hor, R. J. Cava, and M. Z. Hasan, Nature **452**, 970 EP (2008).
- [12] D. Hsieh, Y. Xia, L. Wray, D. Qian, A. Pal, J. H. Dil, J. Osterwalder, F. Meier, G. Bihlmayer, C. L. Kane, Y. S. Hor, R. J. Cava, and M. Z. Hasan, Science **323**, 919 (2009).
- [13] Y. Xia, D. Qian, D. Hsieh, L. Wray, A. Pal, H. Lin, A. Bansil, D. Grauer, Y. S. Hor, R. J. Cava, and M. Z. Hasan, Nature Physics **5**, 398 EP (2009).
- [14] Y. Chen, J. Analytis, J. H. Chu, Z. Liu, S. K. Mo, X. Qi, H. Zhang, D. Lu, X. Dai, and Z. Fang, Nature Physics **5**, 398 EP (2009).
- [15] M. König, S. Wiedmann, C. Brüne, A. Roth, H. Buhmann, L. W. Molenkamp, X.-L. Qi, and S.-C. Zhang, Science **318**, 766 (2007).
- [16] M. Atala, M. Aidelsburger, J. T. Barreiro, J. Abanin, T. Kitagawa, E. Demler, and I. Bloch, Nature Physics **9**, 795–800 (2013).
- [17] M. Bello, C. E. Creffield, and G. Platero, Scientific Reports **6**, 22562 EP (2016).
- [18] M. Bello, C. E. Creffield, and G. Platero, Phys. Rev. B **95**, 094303 (2017).
- [19] M. Benito, A. Gómez-León, V. M. Bastidas, T. Brandes, and G. Platero, Phys. Rev. B **90**, 205127 (2014).
- [20] Z.-Z. Li, C.-H. Lam, and J. Q. You, Phys. Rev. B **96**, 155438 (2017).
- [21] M. Niklas, M. Benito, K. S., and G. Platero, Nanotechnology **27**, 454002 (2016).
- [22] C. E. Creffield and G. Platero, Phys. Rev. B **69**, 165312 (2004).
- [23] C. E. Creffield, Phys. Rev. Lett. **99**, 110501 (2007).
- [24] D. Zueco, F. Galve, S. Kohler, and P. Hänggi, Phys. Rev. A **80**, 042303 (2009).
- [25] J. Klinovaja, P. Stano, and D. Loss, Phys. Rev. Lett. **116**, 176401 (2016).
- [26] L. Jiang, T. Kitagawa, J. Alicea, A. R. Akhmerov, D. Pekker, G. Refael, J. I. Cirac, E. Demler, M. D. Lukin, and P. Zoller, Phys. Rev. Lett. **106**, 220402 (2011).
- [27] R. Aguado and G. Platero, Phys. Rev. B **55**, 12860 (1997).
- [28] M. Thakurathi, A. A. Patel, D. Sen, and A. Dutta, Phys. Rev. B **88**, 155133 (2013).
- [29] J. Cayssol, B. Dóra, F. Simon, and R. Moessner, physica status solidi (RRL) – Rapid Research Letters **7**, 101.
- [30] N. H. Lindner, G. Refael, and V. Galitski, Nature Physics **7**, 490 (2011).
- [31] T. Oka and H. Aoki, Phys. Rev. B **79**, 081406 (2009).
- [32] P. M. Perez-Piskunow, G. Usaj, C. A. Balseiro, and L. E. F. F. Torres, Phys. Rev. B **89**, 121401 (2014).
- [33] G. Usaj, P. M. Perez-Piskunow, L. E. F. Foa Torres, and C. A. Balseiro, Phys. Rev. B **90**, 115423 (2014).

- [34] E. Suárez Morell and L. E. F. Foa Torres, *Phys. Rev. B* **86**, 125449 (2012).
- [35] Z. Gu, H. A. Fertig, D. P. Arovas, and A. Auerbach, *Phys. Rev. Lett.* **107**, 216601 (2011).
- [36] P. Delplace, A. Gómez-León, and G. Platero, *Phys. Rev. B* **88**, 245422 (2013).
- [37] M. Busl, G. Platero, and A.-P. Jauho, *Phys. Rev. B* **85**, 155449 (2012).
- [38] P. M. Perez-Piskunow, L. E. F. Foa Torres, and G. Usaj, *Phys. Rev. A* **91**, 043625 (2015).
- [39] A. Gómez-León, P. Delplace, and G. Platero, *Phys. Rev. B* **89**, 205408 (2014).
- [40] A. Gómez-León and G. Platero, *Phys. Rev. Lett.* **110**, 200403 (2013).
- [41] J.-i. Inoue and A. Tanaka, *Phys. Rev. Lett.* **105**, 017401 (2010).
- [42] N. H. Lindner, D. L. Bergman, G. Refael, and V. Galitski, *Phys. Rev. B* **87**, 235131 (2013).
- [43] V. Dal Lago, M. Atala, and L. E. F. Foa Torres, *Phys. Rev. A* **92**, 023624 (2015).
- [44] Y. T. Katan and D. Podolsky, *Phys. Rev. Lett.* **110**, 016802 (2013).
- [45] M. D. Reichl and E. J. Mueller, *Phys. Rev. A* **89**, 063628 (2014).
- [46] I.-D. Potirniche, A. C. Potter, M. Schleier-Smith, A. Vishwanath, and N. Y. Yao, *Phys. Rev. Lett.* **119**, 123601 (2017).
- [47] W. Zheng and H. Zhai, *Phys. Rev. A* **89**, 061603 (2014).
- [48] M. Rechtsman, J. Zeuner, Y. Plotnik, Y. Lumer, D. Podolsky, F. Dreisow, S. Nolte, M. Segev, and A. Szameit, *Nature* **496**, 196 (2013).
- [49] R. Fleury, A. Khanikaev, and A. Alù, *Nature Communications* **7** (2016), 10.1038/ncomms11744.
- [50] Y. Peng, C. Qin, D. Zhao, Y. Shen, X. Xu, M. Bao, H. Jia, and X. Zhu, *Nature Communications* **7** (2016), 10.1038/ncomms13368.
- [51] J. R. Petta, A. C. Johnson, J. M. Taylor, E. A. Laird, A. Yacoby, M. D. Lukin, C. M. Marcus, M. P. Hanson, and A. C. Gossard, *Science* **309**, 2180 (2005).
- [52] K. D. Petersson, J. R. Petta, H. Lu, and A. C. Gossard, *Phys. Rev. Lett.* **105**, 246804 (2010).
- [53] T. H. Oosterkamp, T. Fujisawa, W. G. van der Wiel, K. Ishibashi, R. V. Hijman, S. Tarucha, and L. P. Kouwenhoven, *Nature* **395**, 873 EP (1998).
- [54] F. Martins, F. K. Malinowski, P. D. Nissen, E. Barnes, S. Fallahi, G. C. Gardner, M. J. Manfra, C. M. Marcus, and F. Kuemmeth, *Phys. Rev. Lett.* **116**, 116801 (2016).
- [55] M. D. Reed, B. M. Maune, R. W. Andrews, M. G. Borselli, K. Eng, M. P. Jura, A. A. Kiselev, T. D. Ladd, S. T. Merkel, I. Milosavljevic, E. J. Pritchett, M. T. Rakher, R. S. Ross, A. E. Schmitz, A. Smith, J. A. Wright, M. F. Gyure, and A. T. Hunter, *Phys. Rev. Lett.* **116**, 110402 (2016).
- [56] T. Hensgens, T. Fujita, L. Janssen, X. Li, C. J. Van Diepen, C. Reichl, W. Wegscheider, S. Das Sarma, and L. M. K. Vandersypen, *Nature* **548**, 70 EP (2017).
- [57] A. Y. Smirnov, S. Savell'ev, L. G. Mouroukh, and F. Nori, *EPL (Europhysics Letters)* **80**, 67008 (2007).
- [58] J. Gray, A. Bayat, R. K. Puddy, C. G. Smith, and S. Bose, *Phys. Rev. B* **94**, 195136 (2016).
- [59] D. M. Zajac, T. M. Hazard, X. Mi, E. Nielsen, and J. R. Petta, *Phys. Rev. Applied* **6**, 054013 (2016).
- [60] H. Guo, *Physics Letters A* **378**, 1316 (2014).
- [61] W. P. Su, J. R. Schrieffer, and A. J. Heeger, *Phys. Rev. Lett.* **42**, 1698 (1979).
- [62] B. Pérez-González, M. Bello, A. Gómez-León, and G. Platero, *Phys. Rev. B* **99**, 035146 (2019).
- [63] F. Grossmann, T. Dittrich, P. Jung, and P. Hänggi, *Phys. Rev. Lett.* **67**, 516 (1991).
- [64] A. Eckardt and E. Anisimovas, *New Journal of Physics* **17**, 093039 (2015).
- [65] N. Goldman and J. Dalibard, *Phys. Rev. X* **4**, 031027 (2014).
- [66] V. M. Martinez Alvarez and M. D. Coutinho-Filho, *Phys. Rev. A* **99**, 013833 (2019).
- [67] L. Fu and C. L. Kane, *Phys. Rev. B* **76**, 045302 (2007).
- [68] P. Delplace, D. Ullmo, and G. Montambaux, *Phys. Rev. B* **84**, 195452 (2011).
- [69] P. Nevado, S. Fernández-Lorenzo, and D. Porras, *Phys. Rev. Lett.* **119**, 210401 (2017).
- [70] T. Fujisawa, D. G. Austing, Y. Tokura, Y. Hirayama, and S. Tarucha, *Phys. Rev. Lett.* **88**, 236802 (2002).